Ab Initio Study on Phenylacetylene in S_1 and S_2

Yoshiaki Amatatsu* and Yasunori Hasebe

Faculty of Engineering and Resource Science, Akita University, Tegata Gakuen-cho, Akita 010-8502, Japan

Received: June 1, 2003; In Final Form: September 22, 2003

The electronic structures of phenylacetylene (PA) in S_0, S_1, and S_2 have been examined by means of ab initio complete active space self-consistent field (CASSCF) and the second-order multi-reference Möller−Plesset (MRMP2) calculations. The stable structures of PA in both S_0 and S_1 are optimized to be C_{2v}. The stable structure in S_1 is characterized as an enlarged benzene ring, which is caused by local $\pi-\pi^*$ excitation within the benzene ring. On the other hand, the S_2 geometry is optimized to be a quinoid structure where the aromaticity of the benzene ring is completely lost. To discuss the internal conversion from S_2 into S_1, the conical intersection between S_2 and S_1 (S_2/S_1-CIX) has been also determined. The S_2/S_1-CIX is characterized as a quinoid structure in the benzene part and allene-like in the acetylene part. The present computational result well reproduces the experimental findings, such as the rotational constant and the feature of the absorption spectrum.

I. Introduction

The photochemical behaviors of aryl alkenes and alkynes have been of great interest in the basic science of laser spectroscopy as well as in the applied material science. As to a prototype of aryl alkenes, i.e., styrene (STY), we recently proposed a new picture of the photochemical behavior.[1−3] In the present study, we theoretically examine the photochemical behavior of a prototype of aryl alkynes, phenylacetylene (PA), and compare it with that of STY previously reported. In the following paragraphs, we make a brief review on the previous studies on PA.

The stable geometry in S_0 was of main interest in the early days of the research. It is found that the stable PA in S_0 is C_{2v} geometry by means of microwave and electron diffraction experiments.[4,5] The force field analysis of the infrared and Raman spectra also support the validity of the C_{2v} structure.[6,7] This experimental finding was confirmed by means of ab initio calculations.[5,8−10]

The study on the low-lying excited states of PA stemmed from the work by King and So.[11] They measured the absorption spectrum and found three absorption bands (279−270, 239−220, and 194−190 nm), whose intensities increase in energy. The first weak absorption band is rich in a rotational structure to be analyzed. The second absorption band is diffuse with prominent twin peaks. They made comment that the second absorption band with a peculiar intensity distribution is unlikely to correspond to separate electronic transition and tentatively pointed out that this is due to the predissociation of the system of PA. The third absorption, which is not our present interest, is also structureless and is supposed to be in relation to the decomposition process of PA.[12]

The seminal works by King and So about the first and second absorption bands were developed by the following works. Swiderek et al. performed low-energy electron energy loss spectroscopy so as to assign the weak peak at 4.41 eV and the intense absorption around 5.05−5.30 eV to the S_0-S_1 0−0 and the S_0-S_2 transitions, respectively.[13] Smalley and co-workers measured a dispersed fluorescence spectrum so that the S_1 with B_2 symmetry under the C_{2v} point group is the locally excited $\pi-\pi^*$ within the benzene ring.[14] Several authors confirmed their assignment of S_1 by means of vibrational force field analyses.[15−18] Tzseng and co-workers performed the resonant two-photon ionization studies to discuss the electronic and geometrical structures in S_1. By combining ab initio single excitation calculations (CIS) with their experimental results, they concluded that S_1 has a quinoid structure where the aromaticity of the benzene ring is lost.[10] Pratt and co-workers measured the rotationally resolved fluorescence spectra so as to find out PA in S_1 is polarized along the *b* axis and pointed out that a CIS calculation gives a result of the *a* axis being polarized.[19]

Contrary to the richness of the information on the S_1 state, the discussion on the second absorption band with a peculiar shape is very limited. Vaida et al. examined it by means of the direct absorption spectroscopy.[20] They found the characteristic 1846 ± 15 cm^{-1} interval of the vibrational mode and tentatively assigned it the stretching vibration relating to the triple bond.

Despite much effort to elucidate the photochemistry of PA in S_1 and S_2, it is still controversial or unclear. So our present purpose is to examine both electronic and geometrical structures in S_1 and S_2 by means of a reliable ab initio method.

The present paper is organized as follows. In the next section, we describe the method of calculations based on preliminary configuration interaction (CI) results. In section III, we mention the electronic and geometrical structures of PA in S_1 and S_2 as well as S_0. Then we discuss the mechanism of the internal conversion from S_2 into S_1. We also compare the photochemistry of PA with that of STY. Finally, we give a summary on the present computational results.

II. Method of Calculations

The global potential energy surfaces of PA by means of complete active space self-consistent field (CASSCF) and the second-order multi-reference Möller−Plesset (MRMP2) calculations are desirable to do a reliable discussion on the photochemical behavior of PA. To obtain the global potential energy surfaces, however, we have to perform the calculations at many geometrical points, which include not only the Franck−Condon

* To whom correspondence should be addressed. E-mail:amatatsu@ipc.akita-u.ac.jp. Fax: 81-18-889-2601.

10.1021/jp0355253 CCC: $25.00
Published on Web 11/19/2003

(FC) region but also the region far away from the FC region such as a conical intersection (CIX). Therefore, how to reduce the computational labor is important. Our strategy for the calculation of a global potential energy surface of PA is as follows. In the first step, we did CI calculations at various geometries which covered the conformations possible to contribute to the photochemical process of PA. In the preliminary CI calculations, it was found that at all of the conformations sampled here, the low-lying excited states are well described by the CSFs (configuration state functions) arising from the highest four π to the lowest four unoccupied π^* orbitals. This implies that the 8 electrons in 8 orbitals CASSCF ((m,n) CASSCF in general) and its MRMP2 are enough to discuss the photochemistry of PA. However, the nature of the set of highest four orbitals in active space is dependent on the conformation. In other words, the remaining fifth π occupied orbital (i.e., the lowest occupied π orbital) which is out of the active space at a conformation slips in a set of the active orbitals at another conformation. Generally speaking, the active space which is dependent on the conformation leads to unphysical discontinuity of the potential energy surfaces. To avoid it, the additional fifth occupied π orbital is included in the active space. That is, we adopted (10,9)CASSCF and MRMP2 for the scanning of the global potential energy surfaces.

First, we optimized the equilibrium geometry of S_0 (S_0-geometry) of PA by means of a state-specific (10,9)CASSCF method. Then we examined the electronic structures at the S_0-geometry by means of a state specific (10,9)CASSCF and its MRMP2. To discuss the photochemical behavior of PA, we optimized the geometries of S_1 (S_1-geometry) and S_2. The optimization of the S_2 geometry was done under constraint of the planar structure (S_2-planar). We additionally optimized the conical intersection between S_2 and S_1 (S_2/S_1-CIX) to discuss the internal conversion from S_2 into S_1. Because of the limitation of our computer facility, the S_2/S_1-CIX was determined by (8,8)CASSCF method. However, this approach is reasonable because the low-lying excited states (especially S_2 and S_1) in the region around the S_2/S_1-CIX is well described by the CSFs arising from the highest four occupied into the lowest unoccupied orbitals, as mentioned above. We, of course, checked the validity of the truncation of the active space, as mentioned in the next section. In the scanning of the potential energy surfaces for the internal conversion from S_2 into S_1, the molecular orbitals (MOs) were determined by means of a state-specific CASSCF. The basis set used in the present calculations is the Huzinage−Dunning double-ζ (DZ) basis set augmented by polarization ($\alpha_d = 0.75$) on carbon atoms. In the present ab initio calculations, we used the GAMESS program,[21] except for the determination of the S_2/S_1-CIX by Gaussian 98.[22]

III. Results and Discussions

We begin with mentioning the electronic structures of PA at S_0-geometry. S_0-geometry was optimized to be C_{2v} symmetry. In Table 1, we listed the excitation energies, the oscillator strengths, and the main CSFs of each electronic state by means of MRMP2 as well as other methods. The S_1 state with B_2 symmetry under C_{2v} point group can be assigned to the local $\pi-\pi^*$ excitations within the benzene ring, which is well described by a linear combination of the single excitation CSFs of (HOMO-1)-LUMO and HOMO−(LUMO+1) (HOMO, highest occupied MO; LUMO, lowest unoccupied MO). The S_2 state with A_1 symmetry can be assigned to the $\pi-\pi^*$ excitation originated from the HOMO−LUMO single excitation. In Figure 1, the relevant MOs are shown to see what type of MOs contribute to S_1 and S_2. The calculated excitation energies and the oscillator strengths are in agreement with the experimental absorption spectrum.[11] That is, the first absorption (279 nm, i.e., 4.444 eV) is weak, whereas the second one (239 nm, i.e., 5.188 eV) is strong.

TABLE 1: Excitation Energies, Oscillator Strengths and the Main CSFs of PA Excitation Energy (in eV) Oscillator Strength Main CSFs[a]

	excitation energy (eV)	oscillator strength	main CSFs[a]
MRMP2[b]			
$S_0(1^1A_1)$[c]	0.0		0.936(closed shell)
$S_1(1^1B_2)$	4.232	0.001	0.645(2−1′) +0.576(1−2′)
$S_2(2^1A_1)$	5.502	0.234	0.791(1−1′)+0.361(3−1′)
SDT-CI			
$S_0(1^1A_1)$	0.0		0.953(closed shell)
$S_1(1^1B_2)$	5.193	0.002	0.650(2−1′) +0.612(1−2′)
$S_2(2^1A_1)$	6.629	0.230	0.842(1−1′)-0.314(2−2′)
SCI			
$S_0(1^1A_1)$	0.0		1.0(closed shell)
$S_1(1^1B_2)$	6.047	0.002	0.709(2−1′) +0.669(1−2′)
$S_2(2^1A_1)$	6.122	0.126	0.835(1−1′)+0.316(3−3′) −0.364(2−2′)

[a] The CSFs of which absolute values of CI coefficients are greater than 0.3 are listed. Five occupied π orbitals and the lowest four unoccupied π^* ones in the order of energy are designated by 5,4,3,2,1(HOMO),1′(LUMO),2′,3′,4′, respectively. 1−1′ in the parenthesis, for instance, indicates the CSF of single excitation from orbital 1 to 1′. [b] The excitation energies are obtained by means of MRMP2 with (10,9)CASSCF wave function. The oscillator strengths are obtained by means of (10,9)CASSCF. [c] The symmetry label of each electronic state is under C_{2v} geometry.

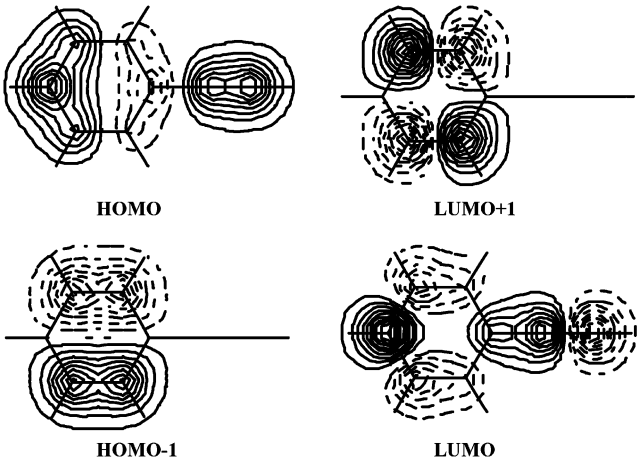

Figure 1. Molecular orbitals relevant to S_1 and S_2 states at S_0-geometry.

Next we mention the optimized geometry of each state in Table 2. The numberings of atoms are shown in Figure 2. The S_0-geometry is optimized to have C_{2v} symmetry. The bond distance of $C^{\alpha}\equiv C^{\beta}$ (1.216 Å) is calculated to be very similar to that of a normal C≡C triple bond. On the other hand, the linkage bond of C^1-C^{α} (1.448 Å) is slightly shorter than a normal C−C single bond, which is ascribed to somewhat resonance between the phenyl group and the triple bond of $C^{\alpha}\equiv C^{\beta}$. Furthermore, the C−C bond distances of the phenyl group (ca. 1.40Å) take intermediate values between normal single and double bond distances, which are close to that of aromatic benzene. These features are in good agreement with the experimental value as well as the previous computational ones at restricted Hartree−Fock (HF) level.[5,8−10] The S_1-geometry is also optimized to be C_{2v} symmetry. The most characteristic point of the S_1 geometry (see Table 1) is that the benzene rings enlarges. This can be

TABLE 2: Characteristic Optimized Parameters of PA

	S_0	S_1	S_2-planar	S_2/S_1-CIX
Bond Distances (in Å)				
$R(C^{\alpha}-C^{\beta})$	1.216	1.210	1.281(1.260)[a]	1.338
$R(C^1-C^{\alpha})$	1.448	1.417	1.358 (1.373)	1.358
$R(C^1-C^2)$	1.395	1.446	1.456 (1.446)	1.482
$R(C^2-C^3)$	1.395	1.438	1.372 (1.372)	1.370
$R(C^3-C^4)$	1.398	1.432	1.445 (1.405)	1.411
$R(C^4-C^5)$	1.398	1.432	1.445 (1.405)	1.411
$R(C^5-C^6)$	1.395	1.438	1.372 (1.372)	1.370
$R(C^{\beta}-H^{\beta})$	1.059	1.059	1.058 (1.054)	1.080
bond Angles (in Degree)				
$\alpha(<C^1C^{\alpha}C^{\beta})$	180.0	180.0	180.0	179.7
$\alpha(<C^{\alpha}C^{\beta}H^{\beta})$	180.0	180.0	180.0	121.3
Dihedral Angles (in Degree)				
$<C^1C^{\alpha}C^{\beta}H^{\beta}$				180.0

[a] The values in the parentheses are those in S_1 taken from ref 10.

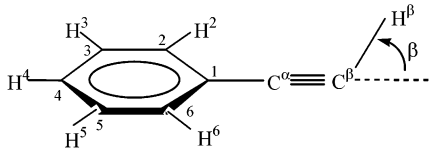

Figure 2. Numbering of atoms in phenylacetylene.

TABLE 3: Relative Energies (in eV) at the Important Conformations

	S_0-geometry	S_1-geometry	S_2(planar)	S_2/S_1-CIX
S_0	0.0			
S_1	4.232	3.980	4.265	5.218
S_2	5.503		5.230	5.022

TABLE 4: Rotational Constants (in MHz) of PA in S_0, S_1, and S_2

state	constant	ab initio	experiment[a]
S_0	A	5670.70(5763.51)[b]	5681.5
	B	1512.88 (1602.99)	1529.8
	C	1194.26 (1214.76)	1204.9
S_1	A	5419.84	5459.6
	B	1479.73	1505.1
	C	1162.37	1179.9
S_2(planar)	A	5241.01 (5567.44)	
	B	1511.98 (1528.94)	
	C	1173.45	

[a] The values are taken from ref 19. [b] The values in parentheses are those in S_1 taken from ref 10.

ascribed to the local $\pi-\pi^*$ excitation within the benzene ring. That is, the occupied π electrons in the benzene ring are excited into unoccupied π^* orbitals, which leads to a weakening and lengthening of the relevant C−C bonds in the benzene ring. This feature is found in that of styrene in S_1.[2] As seen in Table 3, the energy at the S_1-geometry (3.980 eV) is lower than that at the S_0-geometry (4.232 eV). This implies that the S_1 state characterized above is stable in the FC region with a long lifetime. Actually, PA in S_1 has a long fluorescence lifetime of 43 ns. We justify the feature of the enlargement of the benzene ring by comparing the calculated rotational constants with the experimental ones.[19] In Table 4, we listed the computational and experimental rotational constants in S_0 and S_1. It can be seen that they are in good agreement with each other. The remarkable decrease of ΔA in S_1 can be interpreted as the enlargement of the benzene ring.

We turn to discuss the geometrical feature of S_2 in relation to the electronic structure. S_2-planar which is optimized under constraint of the planar is characterized as a quinoid structure with C_{2v} symmetry. The aromaticity of the benzene ring is completely lost. The bond distances of C^2-C^3 and C^5-C^6 becomes shorter than a normal C−C bond distance of aromatic benzene ring and closer to a normal C=C double bond, whereas the other becomes closer to a normal C−C single bond. The linkage bond distance of C^1-C^{α} more shrinks to a normal C=C double bond, whereas the bond distance of $C^{\alpha}-C^{\beta}$ elongates from a C≡C triple bond to a C=C double bond. In other words, the part of $C^1C^{\alpha}C^{\beta}$ prefers to take an allene-like ($C^1=C^{\alpha}=C^{\beta}$) structure in S_2 rather than the structure of $C^1-C^{\alpha}\equiv C^{\beta}$. This geometrical change of the $C^1C^{\alpha}C^{\beta}$ part can be explained in terms of the nature of HOMO and LUMO, considering S_2 is well described by HOMO−LUMO single excitation (refer to Figure 1). Upon electronic excitation into S_2, the out-of-plane π bonding orbital around the $C^{\alpha}-C^{\beta}$ bond changes into the antibonding orbital and the π orbital in the linkage bond region changes from antibonding into bonding character. This is an explanation why the part of $C^1C^{\alpha}C^{\beta}$ takes an allene-like structure in S_2. Additionally, the drastic change of this part is suggestive to discuss the shape of the S_2 potential energy surface around the S_2-planar. That is, the electronic excitation into S_2 causes the change of the hybridizations of the carbon atom C^{β} from sp into sp^2. As a consequence, H^{β} is preferable to be located out of the plane spanned by the remaining part. In other words, S_2-planar is expected to be unstable with respect to the $<H^{\beta}C^{\beta}C^{\alpha}$ out-of-plane bending motion, which will be mentioned in detail later.

Here it may be worthwhile making comment on the difference between previous computational results and ours. Tzeng and co-workers performed the geometry optimization of S_1 by means of single excitation CI (SCI or CIS in the terminology of the Gaussinan package) so as to obtain a quinoid stable structure in S_1, which is similar to our S_2-planar.[10] They mentioned that their S_1 geometry well reproduces the rotational constants in S_1, though our result at S_1-geometry characterized as an enlarged benzene ring is much better (see Table 4). To check the difference, we performed two types of CI calculations at S_0-geometry, i.e., SCI and SDT-CI, where the CSFs up to triple excitations from the closed-shell HF configuration are included. The results are also listed in Table 1. The SDT-CI results are in qualitative agreement with the present MRMP2 results. That is, the main CSFs, oscillator strengths and the energy difference between S_2 and S_1 are similar to those by the more sophisticated method of MRMP2. In the SCI results, on the other hand, the electronic states of S_1 and S_2 are very close to each other around the FC region. So the excited state of which stable geometry is a quinoid stable structure may be S_1 at their geometry optimization step by means of SCI. Furthermore, SCI results cannot explain the experimental absorption spectrum. Even in our SCI calculation, S_1, whose absorption intensity is weak, is not well separated by S_2 with strong intensity. This is not in agreement with the experimental findings.[11] Pratt et al. also pointed out the difference between SCI result and their experimental finding.[19] They found that S_1 is *b*-axis polarized, whereas S_1 by SCI is *a*-axis polarized because of the HOMO−LUMO single excitation. Therefore, we conclude that the SCI calculation is possible to give a wrong order among the excited states and the multiple excitations, inherently neglected in SCI calculations, are important to properly describe the local $\pi-\pi^*$ excited state within the benzene ring.

Again we are back to discuss the photochemistry of PA based on our present calculations. The next concern is the internal conversion from S_2 into S_1. So we did an optimization of the S_2/S_1-CIX. The characteristic optimized parameters are also listed in Table 2. Most of the parameters are similar to those of

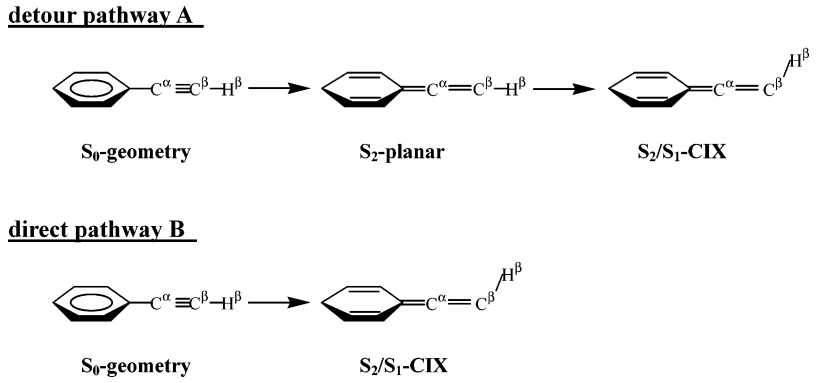

Figure 3. Schematic representation of possible internal conversion from S_2 into S_1.

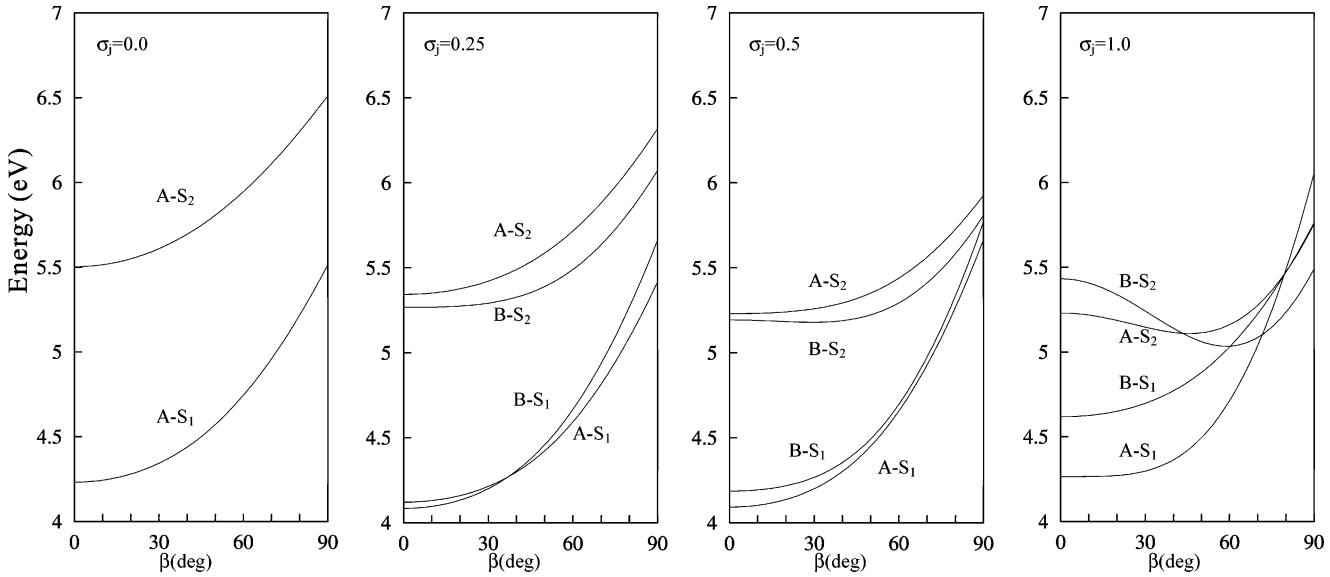

Figure 4. Potential energy curves with respect to the $C^{\beta}-H^{\beta}$ out-of-plane mode (β) by MRMP2 with (10,9)CASSCF wave function. Glossary of $A-S_1$, for instance, means the potential energy curve of S_1 at a given σ_A.

TABLE 5: Relative Energies and the Main CSFs at S_2/S_1-CIX

	relative energy (in eV)[a]	main CSFs[b]
S_1	5.218	$0.610(2-1') + 0.581(1-2')$
S_2	5.022	$0.884(1-1')$

[a] The values are obtained by means of MRMP2 with the (10,9)CASSCF wave function. [b] The CSFs of which absolute values of CI coefficients are greater than 0.3 are listed. Five occupied π-orbitals and the lowest four unoccupied π^*-ones in the order of energy are designated by 5,4,3,2,1(HOMO),1′(LUMO),2′,3′,4′, respectively. $1-1'$ in the parenthesis, for instance, indicates the CSF of single excitation from orbital 1 to 1′.

S_2-planar characterized as a quinoid structure. However, the following two are different from those of S_2-planar. One is the bending angle of $<H^{\beta}C^{\beta}C^{\alpha}$ (121.3, not 180 of S_2-planar). The other is the allene part of $C^1{=}C^{\alpha}{=}C^{\beta}$. That is, at the S_2/S_1-CIX, the two bond distances (C^1-C^{α} and $C^{\alpha}-C^{\beta}$) are similar to each other, which is found in many allenoid molecules in S_0. These support that the partial structure of $C^1C^{\alpha}C^{\beta}H^{\beta}$ is allene-like, as rationalized above. In Table 5, we listed the energy and the main CSFs by means of MRMP2 with (10,9)-CASSCF wave function at the (8,8)CASSCF S_2/S_1-CIX geometry. It can be seen that both electronic structures in S_1 and S_2 are still similar to the characters in the FC region but the energy difference between S_2 and S_1 is small enough to be a CIX. This implies that the S_2/S_1-CIX geometry by means of MRMP2 optimization with the (10,9)CASSCF wave function, which is quite unrealistic level of calculation for the present, is not so different from that of the present (8,8)CASSCF method.

Now we discuss the mechanism of the internal conversion from S_2 into S_1, based on the ingredients of electronic and geometrical structures mentioned in the previous paragraphs. Our concern is about how PA in S_2 travels from the S_0-geometry into S_2/S_1-CIX. There are two promising pathways of "detour pathway A" and "direct pathway B", as shown in Figure 3 schematically. In Figure 4, we show the S_1 and S_2 potential energy curves with respect to the bending angle β (see Figure 2). Here we define a quinoid coordinate which ensures the continuous change of the geometrical parameters from S_0-geometry into S_2-planar or S_2/S_1-CIX. The quinoid coordinates of Q_{iA} and Q_{iB} are expressed by the following:

$$Q_{iA} = (1 - \sigma_A)Q_i(S_0\text{-geometry}) + \sigma_A Q_i(S_2\text{-planar}), \quad 0 \le \sigma_A \le 1$$

$$Q_{iB} = (1 - \sigma_B)Q_i(S_0\text{-geometry}) + \sigma_B Q_i(S_2/S_1\text{-CIX}), \quad 0 \le \sigma_B \le 1$$

In other words, the parameters σ_A and σ_B are a good measure of the extent that the aromaticity of the benzene ring at S_0-geometry is lost. The S_2 potential energy for $\sigma_j = 0$ (j = A and B) (i.e, geometrical parameters are fixed to be those of S_0-geometry except for β) becomes unstable as the increment of β. As increment of σ_j, the S_2 potential curve for σ_B is lower

TABLE 6: Vibrational Frequencies (in cm^{-1}) and L-Matrix Elements of the ν_5 Band[a]

state	geometry	freq[a]	L-matrix elements[b]
S_0	S_0-geometry	2099	0.772($C^{\alpha}C^{\beta}$ str.)-0.559(C^1C^{α} str.)
S_1	S_1-geometry	2065	0.793($C^{\alpha}C^{\beta}$ str.)-0.541(C^1C^{α} str.)
S_2	S_0-geometry($\sigma_B = 0.0$)	1959	0.758($C^{\alpha}C^{\beta}$ str.)-0.572(C^1C^{α} str.)
S_2	$\sigma_B = 0.25$, $\beta = 0°$	1900	0.776($C^{\alpha}C^{\beta}$ str.)-0.576(C^1C^{α} str.)
S_2	$\sigma_B = 0.5$, $\beta = 20°$	1826	0.710($C^{\alpha}C^{\beta}$ str.)-0.624(C^1C^{α} str.)

[a] The force constants in the a_1 block under C_{2v} symmetry are scaled down by 0.82 (relating to C−H stretches) and 0.88 (others), respectively. The absolute values of the coefficients of the L-matrix larger than 0.3 are listed.

than that for σ_A. This means that the direct pathway is more realistic. Incidentally, for $\sigma_B = 0.5$, the S_2 curve becomes flat with respect to β, and for $\sigma_B = 1.0$, two curves of S_1 and S_2 crosses each other at a highly bending angle β so as for PA to relax from S_2 into S_1. On the basis of the above discussion, we can deduce that PA in S_2 travels from S_0-geometry into S_2/S_1-CIX without passing through the S_2-planar (i.e., direct pathway B).

Next we make comment on the peculiar shape of the second absorption band. According to the work on PA in the low-lying excited states by King and So, the second structureless band is related to predissociation.[11] However, our interpretation is different from theirs. Vaida et al. found the characteristic 1846 $\pm$ 15 cm^{-1} interval of the vibrational mode.[20] They tentatively assigned it to the stretching vibration relating to the triple bond. In Table 6, we listed the calculated vibrational frequencies of the ν_5 band (a_1 mode under C_{2v} symmetry) with L-matrix coefficients. It is found that all of the ν_5 bands can be assigned to the coupling vibrational mode between the $C^{\alpha}-C^{\beta}$ and C^1-C^{α} stretches. The ν_5 band in S_0 at the S_0-geometry is calculated to be 2099 cm^{-1} which reproduces the experimental one (2120 cm^{-1}).[6,7] It is a typical triple C−C bond vibrational frequency. The ν_5 band in S_1 at S_1-geometry is calculated to be 2065 cm^{-1}, which is a little smaller than that in S_0. This is due to the resonance between the triple bond and the phenyl part so that the $C^{\alpha}-C^{\beta}$ part loses a bit of its triple bond character. The ν_5 band in S_2 around the FC region, ranging from S_0-geometry at most to $\sigma_B = 0.5$, is much smaller than those of S_0 and S_1 and is in agreement with the experimental one.[20] So we conclude that the peculiar peaks over the broad absorption band is due to the $C^1{=}C^{\alpha}{=}C^{\beta}$ anti-stretch vibration characteristic in the allenoid molecules.

Finally, we point out the similarity of the photochemistry between PA and STY. As to the photochemistry of STY, we recently gave new insights of the photochemical behavior of STY to promote the experimental evidence:[1−3] (i) After the strong transition into S_2, at the initial stage, STY in S_2 prefers to lose the aromaticity of the benzene ring for the photoisomerization; (ii) the S_1/S_0-CIX where the photoisomerization around the ethylenic double bond takes place is a crossing region between zwtterionic and covalent diradical states. The new insight (i) on STY is similar to the present picture on the initial process of PA. That is, the loss of the aromaticity of the benzene ring is essential to the internal conversion from S_2 into S_1 in both PA and STY.

IV. Concluding Remarks

In this paper, we reported on PA in S_1 and S_2 by means of ab initio CASSCF and MRMP2 calculations. Contrary to the previous result by means of SCI calculations, the stable geometry in S_1 is characterized by the enlarged benzene ring. In S_2, on the other hand, the aromaticity of the benzene ring is lost and an allenoid structure of $C^1{=}C^{\alpha}{=}C^{\beta}$ is preferable than a structure of $C^1{-}C^{\alpha}{\equiv}C^{\beta}$, which is similar to optimized geometry of S_1 by previous SCI calculations. The experimental findings of the rotational constants, the vibrational frequencies, and the absorption spectrum can be reasonably interpreted by our present computational results of geometrical features.

Acknowledgment. The numerical calculations were partly performed in the Computer Center of Institute for Molecular Science. This work is financially supported by a Grant-in-Aid for Scientific Research (C) (No. 12640485) and Grant-in-Aid for Scientific Research on Priority Area (A) (Molecular Physical Chemistry) (No. 12042212) from the Ministry of Education, Culture, Sports, Science and Technology.

References and Notes

(1) Amatatsu, Y. *Chem. Phys. Lett.* **2001**, *344*, 200−206.

(2) Amatatsu, Y. *J. Compt. Chem.* **2002**, *23*, 928−937. The review on the photochemistry of styrene is also therein.

(3) Amatatsu, Y. *J. Compt. Chem.* **2002**, *23*, 950−956.

(4) Cox, A. P.; Ewart, I. C.; Stigliani, W. M. *J. Chem. Soc. Fraday Trans. 2* **1975**, *71*, 504−514.

(5) Shultz, G.; Nagy, T.; Portalone, G.; Ramondo, F.; Hargittai, I.; Domenicano, A. *Struct. Chem.* **1993**, *4*, 183−190.

(6) King, G. W.; So, S. P. *J. Mol. Spectrosc.* **1970**, *36*, 468−487.

(7) Singh, K. M.; Thakur, S. N. *Indian J. Phys.* **1995**, *69B*, 407−419.

(8) Császár, A. G.; Fogarasi, G.; Boggs, J. E. *J. Phys. Chem.* **1989**, *93*, 7644−7651.

(9) Martin, P. S.; Yates, K.; Czismadia, I. G. *J. Mol. Struct. (THEOCHEM)* **1989**, *183*, 279−290.

(10) Narayanan, K.; Chang, G. C.; Shieh, K. C.; Tung, C. C.; Tzeng, W. B. *Spectrochim. Acta A* **1996**, *52*, 1703−1716.

(11) King, G. W.; So, S. P. *J. Mol. Spectrosc.* **1970**, *37*, 543−570.

(12) Sorkhabi, O.; Qi, F.; Rizvi, A. H.; Suits, A. G. *J. Am. Chem. Soc.* **2001**, *123*, 671−676.

(13) Swiderek, P.; Göötz, B. *Ber. Bunsen-Ges. Phys. Chem.* **1998**, *102*, 882−893.

(14) Powers, D. E.; Hopkins, J. B.; Smalley, R. E. *J. Chem. Phys.* **1981**, *74*, 5971−5976.

(15) Singh, K. M.; Singh, R. A.; Thakur, S. N. *Indian J. Pure Appl. Phys.* **1997**, *35*, 5−9.

(16) Singh, H.; Laposa, J. D. *J. Lumin.* **1972**, *5*, 32−46.

(17) Bacon, A. R.; Hollas, J. M. *Chem. Phys. Lett.* **1985**, *120*, 477−480.

(18) Chia L.; Goodman, L. *J. Chem. Phys.* **1982**, *76*, 4745−4750.

(19) Ribblett, J. W.; Borst, D. R.; Pratt, D. W. *J. Chem. Phys.* **1999**, *111*, 8454−8461.

(20) Leopold, D. G.; Hemley, R. J.; Vaida, V. *J. Chem. Phys.* **1981**, *75*, 4758−4769.

(21) Schmidt, M. W.; Baldridge, K. K.; Boatz, J. A.; Elbert, S. T.; Gordon, M. S.; Jensen, J.H.; Koseki, S.; Matsunaga, N.; Nguyen, K. A.; Su, S. J.; Windus, T. L.; Dupuis, M.; Montgomery, Jr., J. A. *J. Comput. Chem.* **1993**, *14*, 1347−1363.

(22) Frisch, M. J.; Trucks, G. W.; Schlegel, H. B.; Scuseria, G. E.; Robb, M. A.; Cheeseman, J. R.; Zakrzewski, V. G.; Montgomery, J. A., Jr.; Stratmann, R. E.; Burant, J. C.; Dapprich, S.; Millam, J. M.; Daniels, A. D.; Kudin, K. N.; Strain, M. C.; Farkas, O.; Tomasi, J.; Barone, V.; Cossi, M.; Cammi, R.; Mennucci, B.; Pomelli, C.; Adamo, C.; Clifford, S.; Ochterski, J.; Petersson, G. A.; Ayala, P. Y.; Cui, Q.; Morokuma, K.; Malick, D. K.; Rabuck, A. D.; Raghavachari, K.; Foresman, J. B.; Cioslowski, J.; Ortiz, J. V.; Stefanov, B. B.; Liu, G.; Liashenko, A.; Piskorz, P.; Komaromi, I.; Gomperts, R.; Martin, R. L.; Fox, D. J.; Keith, T.; Al-Laham, M. A.; Peng, C. Y.; Nanayakkara, A.; Gonzalez, C.; Challacombe, M.; Gill, P. M. W.; Johnson, B. G.; Chen, W.; Wong, M. W.; Andres, J. L.; Head-Gordon, M.; Replogle, E. S.; Pople, J. A. *Gaussian 98*, revision A.7; Gaussian, Inc.: Pittsburgh, PA, 1998.